http://communications.science.ankara.edu.tr

Commun.Fac.Sci.Univ.Ank.Ser. A2-A3
Volume 66, Number 2, Pages 228–241 (2024)
DOI:10.33769/aupse.1434783
ISSN 1303–6009 E-ISSN 2618–6462

Research Article; Received: March 12, 2024; Accepted: July 12, 2024

SEARCH POTENTIAL OF THE HIGH ENERGY-LARGE HADRON COLLIDER FOR SPIN-1/2 EXCITED QUARKS IN DI-JET FINAL STATE

Yusuf Oguzhan GÜNAYDIN[1], Mehmet SAHIN[2] and Leyla AYDIN[1]

[1]Department of Physics, Kahramanmaras Sütcü Imam University, Kahramanmaras, TÜRKİYE
[2]Department of Computer Engineering, Usak University, Usak, TÜRKİYE

Abstract. Composite models, which suggest a possible substructure of fundamental particles, can be directly proven by the discovery of the excited quark. Higher energy and higher-luminosity particle colliders are needed to discover the composite structure predicted in the proposed models. The High Energy Large Hadron Collider (HE-LHC) has the potential to be a possible discovery machine for composite models. In this collider, with a center-of-mass energy of 27 TeV and integrated luminosity between 750 and 15000 fb^{-1}, we calculated the exclusion, observation, and discovery limits for the mass of spin-1/2 excited quark in the *di-jet* final state, as well as the attainable compositeness scale values. In addition to these calculations, we scanned free parameters from 0.06 to 1 to determine the HE-LHC potential to reveal spin-1/2 excited quark.

1. Introduction

The Standard Model (SM) is a theory that best describes the interactions between fundamental particles and largely explains the dynamics of these interactions. However, SM cannot provide a sufficient answer to problems such as hierarchy problems, number of families, parameter excess, matter-antimatter asymmetry, quark-lepton symmetry, repetition of fermions, neutrino oscillations, and dark matter. For these problems that particle physicists are trying to solve, new models called Beyond the Standard Model (BSM) theories have emerged. Composite Models are another area of research that predicts the possibility of a substructure of fermions among BSM theories. As research publications that form the basis of Composite Models,

Keywords. Excited quark, HE-LHC, di-jet, particle phenomenology, composite models, compositeness scale.

yusufgunaydin@gmail.com; 0000-0002-0514-6936
mehmet.sahin@usak.edu.tr-Corresponding author; 0000-0001-6777-3938
leylaydiin@gmail.com; 0000-0001-5562-4265.

we can firstly list an article by Low [1] containing the prediction of heavy electrons and muons and the two papers published later by Jogesh C. Pati and Abdus Salam [2,3]. In the last two publications mentioned, they predicted the composite substructure of fermions, which they called "preons." After these groundbreaking studies, extensive research has been conducted in the literature on the compositeness of fermions and bosons [4–15]. Based on these predictions, many researchers have conducted experimental [16–27] and phenomenological [28–53] studies to discover excited fermions, which will directly prove compositeness.

Researchers hypothesize that excited fermions comprise two distinct elementary particle systems, excited quarks ($q^\star$) and excited leptons ($l^\star$), similar to SM fermions. The excited quark can exist in four distinct final states: such as *di-jet* ($q^\star \to jj$), *photon-jet* ($q^\star \to \gamma j$), *W-jet* ($q^\star \to Wj$), and *Z-jet* ($q^\star \to Zj$). Experimentally, some exclusion limits have been imposed on the mass of the excited quark for each final state in the CMS and ATLAS experiments at the European Conseil for Nuclear Research (CERN) with a center-of-mass energy of 13 TeV and total luminosity values of 35.9 fb^{-1} and 139 fb^{-1}, respectively. These experiments' research established mass limits of 6.7 TeV in the *di-jet* final state, 5.5 TeV in the *photon-jet* final state, 5.0 TeV in the *W-jet* final state, and 4.7 TeV in the *Z-jet* final state [27,54,55].

In-depth exploration of BSM theories necessitates particle colliders characterized by elevated center-of-mass energy and exceptionally high integrated luminosity values. CERN plans to establish the HE-LHC in the 2030s with 27 TeV center-of-mass-energy. This new-generation particle collider can provide a comprehensive spectrum for researching excited quarks, boosting a maximum integrated luminosity of 15000 fb^{-1} [56].

The research subject of this study is the discovery (5σ), observation (3σ), and exclusion (2σ) potential of the spin-1/2 excited quark, which transitions to the *di-jet* final state in the HE-LHC using the effective Lagrangian method. In the subsequent sections, we present the interaction Lagrangian, decay widths, cross-section plots, and signal-background analyses of the spin-1/2 excited quark. In the following section, we describe calculations on the discovery, observation, and exclusion mass limits of the spin-1/2 excited quark in the *di-jet* final state at the HE-LHC. Additionally, we discuss the attainable compositeness scale, a crucial parameter in compositeness studies. Furthermore, we analyzed the impact of the spin-1/2 excited quark on the discovery, observation, and exclusion limits by systematically scanning the free parameters that the precise numerical values are unknown. In the last part, the findings are interpreted and discussed.

2. Materials and Methods

2.1. **Interaction Lagrangian.** In the numerical calculations, we utilized the LanHEP [57] software to incorporate the effective Lagrangian of the spin-1/2 excited quark [47,58] (Equation 1) into the CalcHEP [59] simulation software. Using the simulation software, we calculated the decay width and cross-section values for the spin-1/2 excited quark in the *di-jet* final state.

$$L_{eff} = \frac{1}{2\Lambda}\overline{q_R^{\star}}\,\sigma^{\mu\nu}[g_s f_s \frac{\lambda_a}{2} G^a_{\mu\nu} + g f \frac{\overrightarrow{\tau}}{2}\overrightarrow{W}_{\mu\nu} + g^{'} f^{'} \frac{\Upsilon}{2} B_{\mu\nu}]q_L + h.c. \tag{1}$$

In Equation 1, Λ represents the compositeness scale, $q_R^{\star}$ represents the right-handed excited quark, and q_L represents the left-handed SM quark. In addition, the symbols $g,\ g_s,$ and g' represent the gauge coupling constants, and the field strength tensors SU(3), SU(2), and U(1) are represented by the symbols $G^a_{\mu\nu}$, $\vec{W}_{\mu\nu}$, and $B_{\mu\nu}$, respectively. The remaining parameters are expressed as Gell-Mann matrices λ_a, Pauli spin matrices $\vec{\tau}$, weak hyper-charge Υ, and dimensionless free parameters $f_s,\ f$ and f'.

2.2. **Decay Widths and Cross Sections.** Excited quarks may consist of three families, like the SM quarks. The parton distribution functions of the u quark and gluon inside the proton are more dominant than those of other quarks, so in proton-proton colliders, the most dominant production process of excited quarks occurs as $gu \to u^{\star} \to gu$. As a result, first-family excited quarks will have a higher production cross-section. In contrast, the production cross sections of the second and third family excited quarks, which can be produced in the proton-proton collider through the SM quark-gluon-excited quark vertices corresponding to their respective families, will be much smaller. As an exception to these statements, it can be shown that excited quarks can make transitions between families through the Flavor Changing Neutral Current (FCNC) interactions. Experimentally, it is evident that an FCNC interaction between SM quarks has not been observed at the tree level. Excited quarks entering the FCNC interactions with the SM quarks can cause more complex phenomenological final states. For these reasons, second and third-family excited quark productions and the FCNC interactions of excited quarks with the SM quarks are excluded from the scope of this study. So, this study focused exclusively on examining excited quarks that interact with the first-family quarks of the SM. For excited quarks, (1) excited quark $u^{\star}$ if $\mathrm{m_{u^\star}} > \mathrm{m_{d^\star}}$, (2) excited quark $d^{\star}$ if $\mathrm{m_{d^\star}} > \mathrm{m_{u^\star}}$, and (3) excited quark $q^{\star}$ states if $\mathrm{m_{u^\star}} = \mathrm{m_{d^\star}}$ (degenerate) were investigated. In addition, (a) Λ = 27 TeV and (b) $\Lambda = \mathrm{m_{Q^\star}}$ values were used in the compositeness scale we used in our calculations ($\mathrm{Q}^{\star} : u^{\star},\ d^{\star}$, and $q^{\star}$). We performed decay width and cross-section calculations, considering the experimentally determined exclusion mass limit of 6.7 TeV for the excited quark in the *di-jet* final state by selecting free parameters as $f = f_s = f' = 1$. For the (a) and (b) preferences of the compositeness scale, the decay width graphs of the excited d quark ($d^{\star}$) and the excited u quark ($u^{\star}$) contributed by the total and four different channels separately are given in Figures 1 and 2, respectively. In these plots, we observe that the *di-jet* final state contributes the most to the decay widths of the excited u and d quarks.

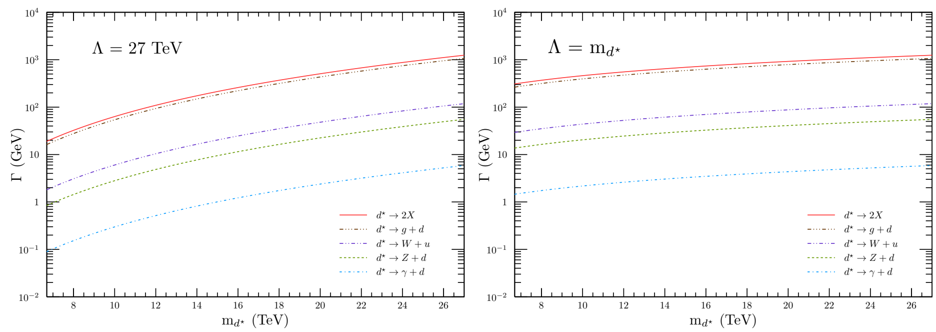

FIGURE 1. Total decay width as a function of spin-1/2 excited d quark for $\Lambda = 27$ TeV (left panel) and $\Lambda = \mathrm{m_{d^\star}}$ (right panel).

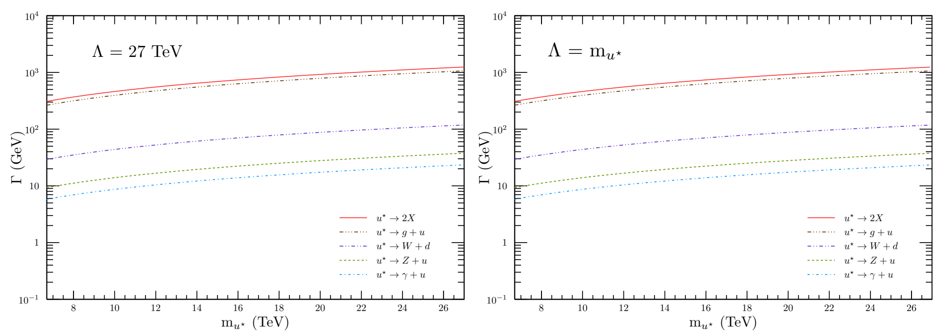

FIGURE 2. Total decay width as a function of spin-1/2 excited u quark for $\Lambda = 27$ TeV (left panel) and $\Lambda = \mathrm{m_{u^\star}}$ (right panel).

To mitigate potential divergences in the cross-section values, we present the cross-section graphs for $d^\star$, $u^\star$, and $q^\star$ by imposing the constraint of $P_{T_j} > 25$ GeV, as illustrated in Figure 3. We selected CT10 for the quark distribution function [60], and in these cross-section calculations, we set the renormalization and factorization scales equal to the mass of the excited quarks. Both plots in Figure 3 depict the cross-section values capable of yielding at least one event, starting from the experimental exclusion value of 6.7 TeV aligned with the mass of excited quarks. This consideration incorporates the maximum anticipated integrated luminosity value for the HE-LHC. The disparity between the two plots arises from employing two distinct values of the compositeness scale. As anticipated, setting the compositeness scale equal to the mass of the excited quark results in a higher cross-section.

2.3. **Signal and Background Analysis.** For the signal, $pp \to u^\star + X \to ug + X$, $pp \to d^\star + X \to dg + X$, and $pp \to q^\star + X \to qg + X$ processes were examined

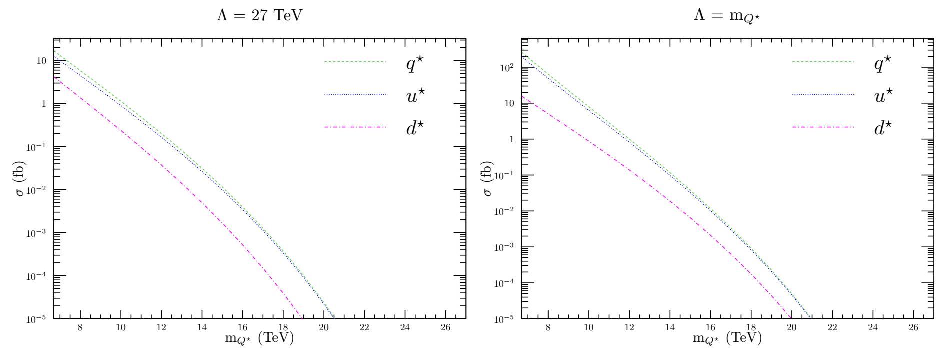

FIGURE 3. Distribution plots in cross-section versus mass for the *di-jet* final state of spin-1/2 excited quarks at $\Lambda = 27$ TeV (left panel) and $\Lambda = m_{Q^\star}$ (right panel).

separately. As background, the $pp \to jj$+X process meets the mentioned signal processes. We defined the j symbol in the background process as $u, \bar{u}, d, \bar{d}, c, \bar{c}, s, \bar{s}, b, \bar{b}$, and g, and performed calculations accordingly in the simulation software. Initially, we imposed a transverse momentum limitation of 25 GeV for the jets in the signals and background calculations. However, under this constraint, it became challenging to distinguish between the signal and background. By obtaining and examining the transverse momentum (P_{T_j}), pseudo-rapidity (η_j), and invariant mass (m_{jj}) distributions, we determined the necessary limitations for these three important parameters that we will use in our later calculations. In Figure 2.3, we present distribution plots for P_{T_j}, η_j, and m_{jj}, featuring only the case where the compositeness scale is equal to the mass of the excited quark ($\Lambda = m_{Q^\star}$), as the $\Lambda = 27$ TeV scenario exhibits a comparable distribution.

Examining the distributions in Figure 2.3, we define the constraints applied in our calculations for P_{T_j}, η_j, and m_{jj}. While determining the P_{T_j} cut from the plot, the value at which the background is suppressed, and the signal unaffected was selected as 2 TeV. It can be seen in the η_j plot that in the cut applied by choosing between -2.5 and 2.5, a large part of the background will be suppressed. When looking at the m_{jj} plot, the region within $m_{Q^\star} - 2\Gamma^\star < m_{jj} < m_{Q^\star} + 2\Gamma^\star$ of the peaks where the signal is higher than the background was selected as an invariant mass cut. Here, $m_{Q^\star}$ represents the individual masses of all degenerate and non-degenerate excited quarks, and $\Gamma^\star$ represents the decay width of excited quarks.

In addition to these three critical constraints, we selected a cone angle radius of $\Delta R > 0.5$ to enhance the distinction of jets in the *di-jet* final state. Utilizing the specified constraints, we computed the discovery, observation, and exclusion limits on the excited quark mass by the Statistical Significance (SS) relation outlined in

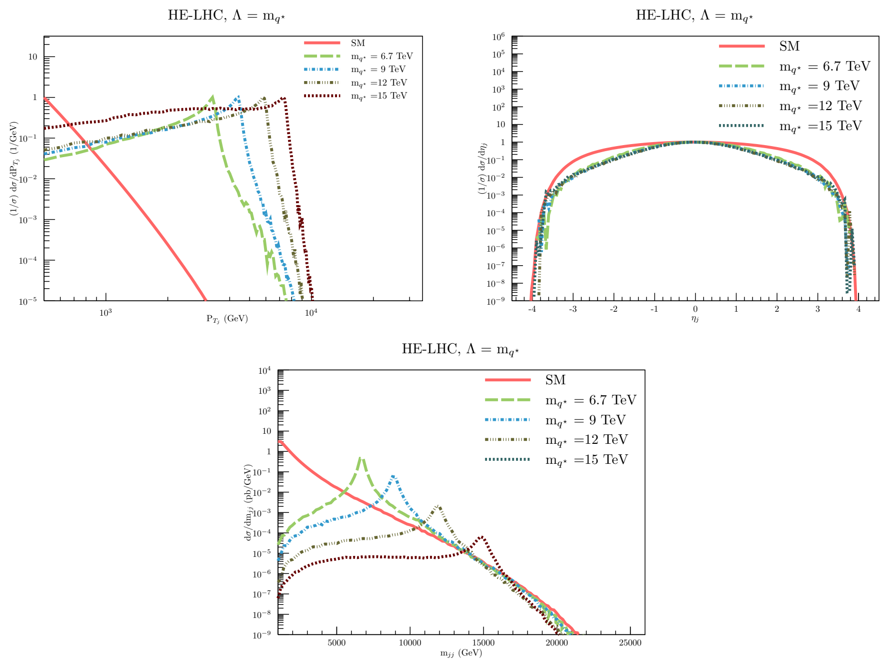

FIGURE 4. Normalized transverse momentum, normalized pseudo-rapidity, and invariant mass distributions of the *di-jet* final-state excited quark for some mass values at HE-LHC.

Equation 2. In this relation, σ_S symbolizes the signal cross section, σ_B symbolizes the background cross section, and $\mathcal{L}_{int}$ represents the integrated luminosity value.

$$SS = \frac{\sigma_S}{\sqrt{\sigma_S + \sigma_B}} \sqrt{\mathcal{L}_{int}} \tag{2}$$

3. Findings and Conclusions

To reveal the ability of the HE-LHC to investigate the spin-1/2 excited quark, firstly, using the cross-section results obtained with the help of CalcHEP simulation software and the statistical significance relation in Equation 2, the spin-1/2 excited quark mass limits were calculated considering the all confidence level 2σ (exclusion), 3σ (observation), and 5σ (discovery). In Table 1, we consider the compositeness scale as 27 TeV. We set the integrated luminosity value for the first year of HE-LHC at 750 fb^{-1}, and we utilize the projected integrated luminosity value of 15000 fb^{-1} for the end of 20 years. The table displays the discovery, observation, and exclusion mass limits for the *di-jet* final state of $d^\star, u^\star$ and $q^\star$. As expected, the mass limits of the spin-1/2 excited quark in the degenerate state were higher. In addition, we observe that the potential exclusion limit for the spin-1/2 $d^{\star}$ *di-jet* final state, which possesses the lowest mass limit in our calculations, is anticipated to significantly surpass the exclusion limit of 6.7 TeV set by the LHC in the first year. As the integrated luminosity value increases, one anticipates that these mass limits will achieve higher values. Although Table 1 numerically presents the statistical significance values when the integrated luminosity reaches 15000 fb^{-1}, Figure 5 illustrates the 20-year developmental trajectory of these mass limits.

TABLE 1. Exclusion, observation, and discovery mass limits obtained with the lowest and highest integrated luminosity values of the HE-LHC for the case where the compositeness scale Λ is taken equal to 27 TeV.

$\mathcal{L}_{int}$ (fb^{-1}) :	750			15000		
SS* :	2σ	3σ	5σ	2σ	3σ	5σ
$m_{d^\star}$ (TeV) :	10.3	9.7	8.8	12.6	12.0	11.2
$m_{u^\star}$ (TeV) :	12.6	11.9	11.1	15.1	14.5	13.6
$m_{q^\star}$ (TeV) :	12.9	12.1	11.5	15.4	14.7	13.9

*SS = Statistical Significance

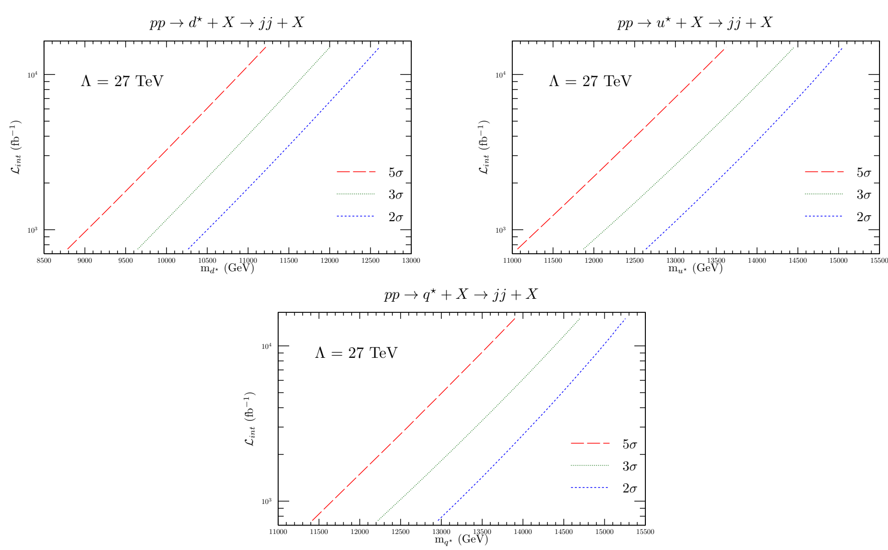

FIGURE 5. Discovery, observation, and exclusion mass limits of the spin-1/2 excited d, u and q quarks in the *di-jet* final state according to the integrated luminosity values of the HE-LHC for $\Lambda = 27$ TeV.

We conducted an additional calculation to determine the mass limit of spin-1/2 excited d, u, and q quarks in the *di-jet* final state at the HE-LHC while considering the compositeness scale taken equal to the mass of the excited quark. The result of our calculations here is higher than the discovery, observation, and exclusion values in the case of $\Lambda = 27$ TeV, as seen in Table 2. Based on the results obtained at this juncture, it is evident that the HE-LHC could achieve an exclusion value significantly surpassing the experimentally imposed exclusion limit on the mass of the excited quark, even within its inaugural year of operation, as seen in Figure 6. These calculations underscore the high potential of the HE-LHC for the discovery of excited quarks.

TABLE 2. Exclusion, observation, and discovery mass limits obtained with the lowest and highest integrated luminosity values of the HE-LHC for the case where the compositeness scale Λ is taken equal to the mass of the excited quark.

$\mathcal{L}_{int}$ (fb^{-1}) :	750			15000		
SS* :	2σ	3σ	5σ	2σ	3σ	5σ
$m_{d^\star}$ (TeV) :	11.7	11.1	10.4	13.6	13.1	12.4
$m_{u^\star}$ (TeV) :	13.8	13.2	12.4	15.9	15.3	14.6
$m_{q^\star}$ (TeV) :	14.0	13.5	12.7	16.0	15.5	14.8

*SS = Statistical Significance

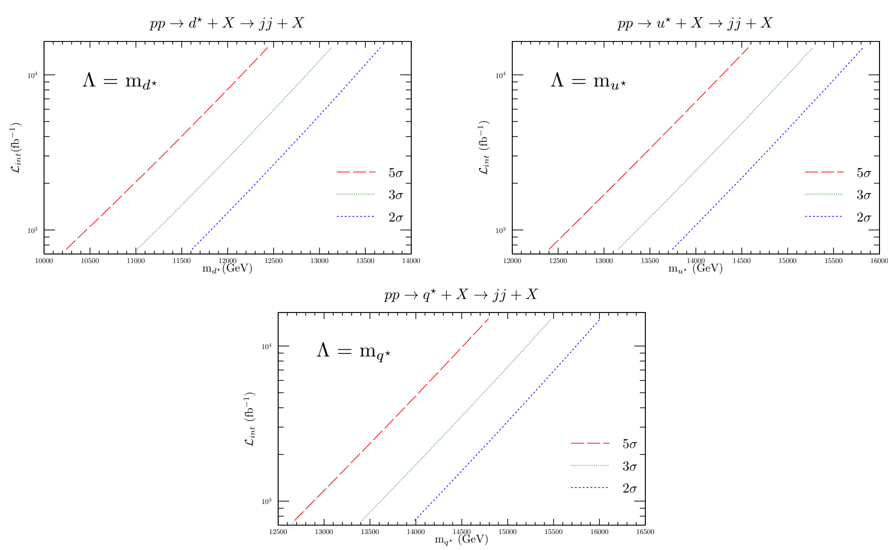

FIGURE 6. Discovery, observation, and exclusion mass limits of the spin-1/2 excited d, u and q quarks in the *di-jet* final state according to the integrated luminosity values of the HE-LHC for $\Lambda = m_{Q^\star}$.

In our analysis thus far, we have equated the compositeness scale, a pivotal parameter in compositeness studies, either to the center-of-mass energy of the particle collider or the mass of the spin-1/2 excited quark. Nevertheless, the compositeness scale remains an indeterminate parameter. To address this issue, we conducted independent calculations to determine the potential compositeness scale limits achievable in the HE-LHC regarding the masses of the spin-1/2 excited quarks in the *di-jet* final state, specifically $d^\star$, $u^\star$, and $q^\star$. Table 3 details our compositeness scale calculations, considering the highest value of the integrated luminosity at HE-LHC, which is 15000 fb^{-1}. We present achievable compositeness scale values corresponding to exclusion, observation, and discovery limits at selected mass values, such as 6.7, 8.7, 10.7, and 12.7 TeV for spin-1/2 $d^\star$, $u^\star$, and $q^\star$ in the *di-jet* final state. At the end of 20 years, when the integrated luminosity value that the HE-LHC will achieve is 15000 fb^{-1}, the exclusion values for the compositeness scale corresponding to masses of 6.7 TeV for $d^\star$, $u^\star$, and $q^\star$ will be 920, 2500, and 3200 TeV, respectively. Figure 7 depicts the compositeness scale scan corresponding to the mass of the *di-jet* final state spin-1/2 excited d, u, and q quarks. Our analysis, initiated from the 6.7 TeV exclusion limit imposed by the LHC on the mass of the excited quark, reveals the potential of the HE-LHC to explore the *di-jet* final state excited quark. Considering our findings, it is conceivable that the HE-LHC might function as a potential discovery machine for excited quarks.

TABLE 3. Achievable compositeness scale values corresponding to some mass values of the excited quark at 15000 fb^{-1} luminosity of the HE-LHC with center-of-mass energy of 27 TeV.

HE-LHC ($\mathcal{L}_{int}$=15000 fb^{-1})									
$m_{Q^\star}$ (TeV)	Λ (TeV)								
	$m_{d^\star}$			$m_{u^\star}$			$m_{q^\star}$		
	5σ	3σ	2σ	5σ	3σ	2σ	5σ	3σ	2σ
6.7	368	614	920	1000	1668	2500	1280	2133	3200
8.7	126	210	314	400	666	999	503	839	1258
10.7	38.4	64	96	145	242	362	179	298	447
12.7	11	18	27	48	80	120	58	96	144

In the calculations thus far, we have set the free parameters to equal one. The value $f = f_s = f' = 1$ is the highest value that free parameters can take, but these parameters can also have values between zero and one. Thus, scanning the numeric value of the free parameters becomes beneficial through the mass of the excited quark. Given that the most extreme value attained in the free parameter scan pertains to the scan for excited q quarks, the results for $d^\star$ and $u^\star$ scans are not incorporated into this study. Figure 8 shows the scans we made considering Λ = 27 TeV and $\Lambda = m_{q^\star}$ according to the mass of the excited q quark. In the calculations involving the scanning of free parameters, we employed an integrated

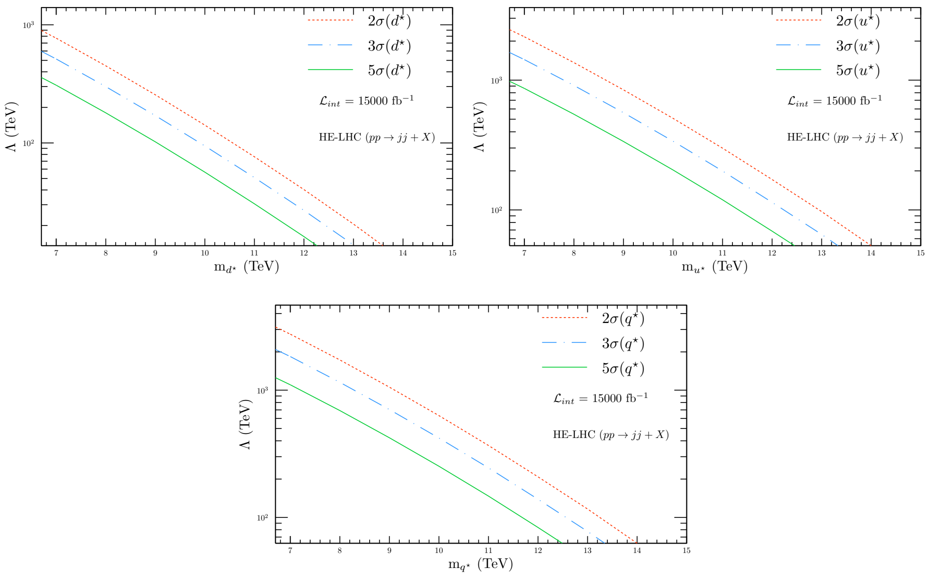

FIGURE 7. Achievable compositeness scale values corresponding to the discovery, observation, and exclusion masses of $d^\star$, $u^\star$ and $q^\star$ when the integrated luminosity value of HE-LHC is 15000 fb^{-1}.

luminosity value of 15000 fb^{-1}, representing the HE-LHC can attain over 20 years. Upon examination of the scan plot for $\Lambda = 27$ TeV, the discovery, observation, and exclusion limits of the excited q quark are apparent, being 6.7 TeV, 8.0 TeV, and 8.8 TeV, respectively, when the free parameters are chosen to 0.13. For the scenario where Λ equals the mass of the excited quark ($\Lambda = \mathrm{m_{q^\star}}$) with the free parameters set to 0.06, the discovery, observation, and exclusion limits of the excited q quark are identified to be 6.7 TeV, 7.5 TeV, and 8.2 TeV, respectively. As depicted in Figure 8, the numerical increase in the value of the free parameters results in an increase in the discovery, observation, and exclusion limits placed on the mass of the excited q quark. The calculations, conducted through a scan of the free parameters and unveiling the potential for values as small as 0.06, indicate the considerable research potential of the HE-LHC for the spin-1/2 excited quark in the *di-jet* final state.

This study encompasses three distinct analyses: determination of discovery, observation, and exclusion limits on the mass of spin-1/2 excited quarks in the *di-jet* final state; assessment of achievable compositeness scale; and screening of free parameters in the context of the High Energy-Large Hadron Collider, taking into account two separate integrated luminosity values. The outcomes of these analyses reveal that the HE-LHC exhibits a significantly greater potential than the LHC in

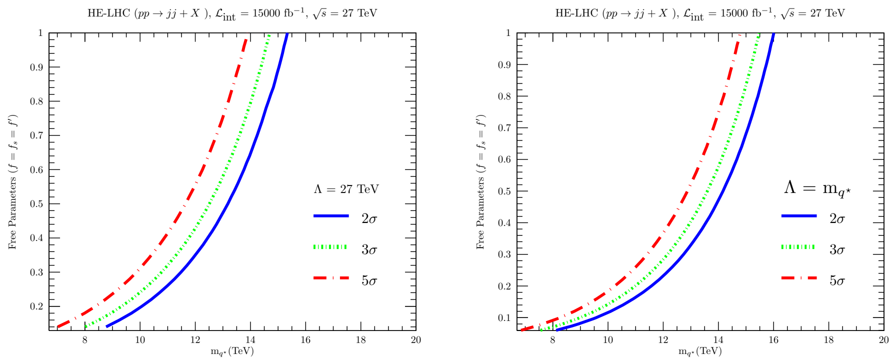

FIGURE 8. In the cases $\Lambda = 27$ TeV (left panel) and $\Lambda = \mathrm{m}_{q^\star}$ (right panel), the attainable mass of $q^\star$ according to the free parameter values limits.

achieving higher limits for the mass of excited quarks, larger values for achievable compositeness scale, and distinctly small values for free parameters.

Author Contribution Statements Authors are equally contributed to the paper. All authors read and approved the final copy of the manuscript.

Declaration of Competing Interests The authors did not receive support from any organization for the submitted work. The authors have no relevant financial or non-financial interests to disclose.

Acknowledgement We thank Usak University, Energy, Environment and Sustainability Application and Research Center for supporting this study.

REFERENCES

[1] Low, F. E., Heavy electrons and muons, *Phys. Rev. Lett.*, 14 (7) (1965), 238–239, https://doi.org/10.1103/PhysRevLett.14.238.
[2] Pati, Jogesh C. and Salam, A., Lepton number as the fourth "color", *Phys. Rev. D*, 10 (1) (1974), 275–289, https://doi.org/10.1103/PhysRevD.10.275.
[3] Pati, J. C., Salam A., and Strathdee, J., Are quarks composite?, *Phys. Lett. B*, 59 (3) (1975), 265–268, https://doi.org/10.1016/0370-2693(75)90042-8.
[4] Terazawa, H., Chikashige, Y., and Akama K., Unified model of the nambu-jona-lasinio type for all elementary-particle forces., *Phys. Rev. D*, 15 (2) (1977), 480–487, https://doi.org/10.1103/PhysRevD.15.480.
[5] Shupe, M. A., A composite model of leptons and quarks., *Phys. Lett. B*, 86 (1979), 87–92, https://doi.org/10.1016/0370-2693(79)90627-0.
[6] Harari, H., A schematic model of quarks and leptons., *Phys. Lett. B*, 86 (1) (1979), 83–86, https://doi.org/10.1016/0370-2693(79)90626-9.
[7] Fritzsch, H. and Mandelbaum G., Weak-interactions as manifestations of the substructure of leptons and quarks., *Phys. Lett. B*, 102 (5), (1981), 319–322, https://doi.org/10.1016/0370-2693(81)90626-2.

[8] Terazawa, H., A fundamental theory of composite-particles and fields., *Phys. Lett. B*, 133 (1-2) (1983), 57–60, https://doi.org/10.1016/0370-2693(83)90105-3.
[9] Eichten, E. J., Lane, K. D., and Peskin, M. E., New tests for quark and lepton substructure., *Phys. Rev. Lett.*, 50 (11) (1983), 811–814, https://doi.org/10.1103/PhysRevLett.50.811.
[10] D'Souza, I. A. and Kalman, C. S., *Preons: Models of leptons, quarks and gauge bosons as composite objects*,(1992).
[11] Çelikel, A., Kantar, M., and Sultansoy, S., A search for sextet quarks and leptogluons at the LHC, *Phys. Lett. B*, 443 (1-4) (1998), 359–364, https://doi.org/10.1016/s0370-2693(98)01299-4.
[12] De Souza, M. E., Weak decays of hadrons reveal compositeness of quarks., *Sci. Ple.*, (6), (2008), https://www.scientiaplena.org.br/sp/article/view/612.
[13] Terazawa, H. and Yasue, M., Excited gauge and higgs bosons in the unified composite model., *Nonlin. Phenom. Complex Syst.*, 19 (1) (2016), 1–6.
[14] Fritzsch, H., Composite weak bosons at the large hadronic collider., *Mod. Phys. Lett. A*, 31 (20) (2016), 1630019, https://doi.org/10.1142/S0217732316300196.
[15] Kaya, U., Oner, B. B., and Sultansoy, S., A minimal fermion-scalar preonic model., *Turkish J. of Phys.*, 42 (3) (2018), 235–241, https://doi.org/10.3906/fiz-1710-28.
[16] Adloff, C. et al., A search for excited fermions at HERA, *Eur. Phys. J. C*, 17 (4) (2000), 567–581, https://doi.org/10.1007/s100520000503.
[17] Acciarri, M. et al., Search for excited leptons in e^+e^- interactions at s=192–202 GeV, *Phys. Lett. B*, 502 (1-4) (2001), 37–50, https://doi.org/10.1016/s0370-2693(01)00133-2.
[18] Chekanov, S. et al., Searches for excited fermions in ep collisions at HERA, *Phys. Lett. B*, 549 (1-2) (2002), 32–47, https://doi.org/10.1016/s0370-2693(02)02863-0.
[19] Chatrchyan, S. et al., Search for resonances in the dijet mass spectrum from 7 TeV pp collisions at CMS, *Phys. Lett. B*, 704 (3) (2011), 123–142, https://doi.org/10.1016/j.physletb.2011.09.015.
[20] Khachatryan, V. et al., Search for excited quarks in the γ + jet final state in proton-proton collisions at $\sqrt{s}$ = 8 TeV, *Phys. Lett. B*, 738 (2014), 274–293, https://doi.org/10.1016/j.physletb.2014.09.048.
[21] Khachatryan, V. et al., Search for Narrow Resonances Decaying to Dijets in Proton-Proton Collisions at $\sqrt{s}$ = 13 TeV, *Phys. Rev. Lett.*, 116 (7) (2016), 071801, https://doi.org/10.1103/PhysRevLett.116.071801.
[22] Aad, G. et al., Search for new phenomena in dijet mass and angular distributions from pp collisions at $\sqrt{s}$=13 TeV with the ATLAS detector, *Phys. Lett. B*, 754 (2016), 302–322, ://doi.org/10.1016/j.physletb.2016.01.032.
[23] Aad, G. et al., Search for new phenomena with photon+jet events in proton-proton collisions at $\sqrt{s}$ =13 TeV with the ATLAS detector, *JHEP*, 2016 (3) (2016), 41, https://doi.org/10.1007/jhep03(2016)041.
[24] Aaboud, M. et al., Search for new phenomena in dijet events using 37 fb^{-1} of pp collision data collected ar $\sqrt{s}$ = 13 TeV with the ATLAS detector, *Phys. Rev. D*, 96 (5) (2017), 052004, https://doi.org/10.1103/PhysRevD.96.052004.
[25] Sirunyan, A. M. et al., Search for dijet resonances in proton–proton collisions at $\sqrt{s}$ = 13 TeV and constraints on dark matter and other models, *Phys. Lett.*, B769 (2017), 520–542, https://doi.org/10.1016/j.physletb.2017.02.012.
[26] Sirunyan, A. M. et al., Search for narrow and broad dijet resonances in proton-proton collisions at $\sqrt{s}$ = 13 TeV and constraints on dark matter mediators and other new particles, *JHEP*, 2018 (8) (2018), 130, https://doi.org/10.1007/jhep08(2018)130.
[27] Sirunyan, A. M. et al., Search for massive resonances decaying into WW, WZ, ZZ, qZ, and qZ with dijet final states at $\sqrt{s}$ = 13 TeV, *Phys. Rev. D*, 97 (7) (2018), 072006, https://doi.org/10.1103/PhysRevD.97.072006.

[28] Renard, F. M., Excited quarks and new hadronic states, *Il Nuovo Cimento*, 77 (1) (1983), 1–20.
[29] Lyons, L., An introduction to the possible substructure of quarks and leptons. *Prog. Part. Nucl. Phys.*, 10 (1983), 227–304, https://doi.org/10.1016/0146-6410(83)90005-4.
[30] Kuhn, J. and Zerwas, P., Excited quarks and leptons. *Phys. Lett. B*, 147 (1-3) (1984), 189–196, https://doi.org/10.1016/0370-2693(84)90618-X.
[31] Pancheri, G. and Srivastava, Y. N., Weak isospin spectroscopy of excited quarks and leptons. *Phys. Lett. B*, 146 (1-2) (1984), 87–94, https://doi.org/10.1016/0370-2693(84)90649-X.
[32] de Rújula, A., Maiani, L., and Petronzio, R., Search for excited quarks, *Phys. Lett. B*, 140 (3-4) (1984), 253–258, https://doi.org/10.1016/0370-2693(84)90930-4.
[33] Kuhn, J. H., Tholl, H. D., and Zerwas, P. M., Signals of excited quarks and leptons, *Phys. Lett. B*, 158 (3) (1985), 270–275, https://doi.org/10.1016/0370-2693(85)90969-4.
[34] Hagiwara, K., Komamiya, S., and Zeppenfeld, D., Excited lepton production at lep and hera. *Z. Phys. C*, 29 (1) (1985), 115–122, https://doi.org/10.1007/Bf01571391.
[35] Baur, U., Hinchliffe, I., and Zeppenfeld, D., Excited quark production at hadron colliders. *Int. J. Mod. Phys. A*, 02 (04) (1987), 1285–1297, https://doi.org/10.1142/s0217751x87000661.
[36] Spira, M. and Zerwas, P. M., *Excited Quarks and Leptons*, pages 519–529, Springer, (1989).
[37] Jikia, G., Excited quark production at ep and γp colliders, *Nucl. Phys. B*, 333 (2) (1990), 317–334, https://doi.org/10.1016/0550-3213(90)90040-k.
[38] Baur, U., Spira, M. and Zerwas, P. M., Excited-quark and -lepton production at hadron colliders. *Phys. Rev. D*, 42 (3) (1990), 815–824, https://doi.org/10.1103/physrevd.42.815.
[39] Boudjema, F., Djouadi, A., and Kneur, J. L., Excited fermions at e^+e^- and ep colliders. *Z. Phys. C*, 57 (3) (1993), 425–449, https://doi.org/10.1007/bf01474339.
[40] Cakir, O. and Mehdiyev, R., Excited quark production at the CERN LHC. *Phys. Rev. D*, 60 (3) (1999), 034004, https://doi.org/10.1103/PhysRevD.60.034004.
[41] Cakir O., Leror C. and Mehdiyev R., Search for excited quarks with the ATLAS experiment at the CERN LHC: Double jets channel. *Phys. Rev. D*, 62 (11) (2000), 114018, https://doi.org/10.1103/PhysRevD.62.114018.
[42] Cakir, O., Leroy, C., and Mehdiyev, R., Search for excited quarks with the ATLAS experiment at the CERN LHC: *W/Z + jet* channel, *Phys. Rev. D*, 63 (9) (2001), 094014, https://doi.org/10.1103/PhysRevD.63.094014.
[43] Eboli, O. J. P., Lietti, S. M., and Mathews, P., Excited leptons at the cern large hadron collider. *Phys. Rev. D*, 65 (7) (2002), 075003, https://doi.org/10.1103/PhysRevD.65.075003.
[44] Cakir, O., Yilmaz, A., and Sultansoy, S., Single production of excited electrons at future e^+e^-, ep and pp colliders, *Phys. Rev. D*, 70 (7) (2004), 075011, https://doi.org/10.1103/PhysRevD.70.075011.
[45] Cakir, O., Leroy, C., Mehdiyev, R., and Belyaev, A., Production and decay of excited electrons at the LHC. *The Eur. Phys. J. C*, 32 (2) (2004), 1–17, https://doi.org/10.1140/epjcd/s2003-01-005-5.
[46] Cakir, O., and Ozansoy, A., Search for excited spin-3/2and spin-1/2leptons at linear colliders. *Phys. Rev. D*, 77 (3) (2008), 035002, https://doi.org/10.1103/PhysRevD.77.035002.
[47] Baur, U., Hinchliffe, I., and Zeppenfeld, D., Excited quark production at hadron colliders, *Int. J. Mod. Phys. A*, 02 (04) (2012), 1285–1297, https://doi.org/10.1142/s0217751x87000661.
[48] Caliskan, A., Excited neutrino search potential of the FCC-based electron-hadron colliders, *Adv. High Energy Phys.*, 2017 (2017), 1–9, https://doi.org/10.1155/2017/4726050.
[49] Caliskan, A. and Kara, S. O., Single production of the excited electrons in the future FCC-based lepton-hadron colliders, *Int.l J. Mod. Phys. A*, 33 (24) (2018), 1850141, https://doi.org/10.1142/S0217751x18501415.
[50] Caliskan, A. and Kara, S. O. and Ozansoy, A., Excited muon searches at the FCC-based muon-hadron colliders, *Adv. High Energy Phys.*, 2017 (2017), 1–9, https://doi.org/10.1155/2017/1540243.

[51] Günaydin, Y. O., Sahin, M., and Sultansoy, S., Resonance Production of Excited u Quark at FCC-based γp Colliders, *Acta Phys. Polon. B*, 49 (10) (2018), 1763, https://doi.org/10.5506/APhysPolB.49.1763.
[52] Akay, A. N., Günaydin, Y. O., Sahin, M., and Sultansoy, S., Search for Excited u and d Quarks in Dijet Final States at Future pp Colliders, *Adv. High Energy Phys.*, 2019 (2019), 1–11, https://doi.org/10.1155/2019/9090785.
[53] Sahin, M., Aydin, G. and Günaydin, Y. O., Excited quarks production at FCC and SPPC pp colliders, *Int.l J Mod. Phys. A*, 34 (29) (2019), 1950169, https://doi.org/10.1142/S0217751x19501690.
[54] Sirunyan, A. M. et al., Search for excited quarks of light and heavy flavor in γ + jet final states in proton-proton collisions at $\sqrt{s} = 13$ TeV, *Phys. Lett. B*, 781 (2018), 390–411, https://doi.org/10.1016/j.physletb.2018.04.007.
[55] Aad, G. et al., Search for new resonances in mass distributions of jet pairs using 139 fb^{-1} of pp collisions at $\sqrt{s} = 13$ TeV with the ATLAS detector, *JHEP*, 2020 (3) (2020), 145, https://doi.org/10.1007/jhep03(2020)145.
[56] Abada, A. et al., HE-LHC: The High-Energy Large Hadron Collider Future Circular Collider Conceptual Design Report (Volume 4), *Eur. Phys. J. S.T.*, 228 (5) (2019), 1109–1382, https://doi.org/10.1140/epjst/e2019-900088-6.
[57] Semenov, A., LANHEP - a package for automatic generation of feynman rules from the lagrangian. version 3.2, *Comp. Phys. Comm.*, 201 (2016), 167–170, https://doi.org/10.1016/j.cpc.2016.01.003.
[58] Zyla, P. A. et al., Review of particle physics, *Prog. Theo. Exp. Phys.*, 2020 (8), (2020), https://doi.org/10.1093/ptep/ptaa104.
[59] Belyaev, A., Christensen N. D., and Pukhov A., CalcHEP 3.4 for collider physics within and beyond the standard model, *Comp. Phys. Comm.*, 184 (7) (2013), 1729–1769, https://doi.org/10.1016/j.cpc.2013.01.014.
[60] Lai, H-L. , Guzzi, M., Huston, J., Li Z., Nadolsky, P. M., Pumplin, J., and Yuan, C. P., New parton distributions for collider physics, *Phys. Rev. D*, 82 (7) (2010), 074024, https://doi.org/10.1103/PhysRevD.82.074024.